Effects of Heat Generation/Absorption on Magnetohydrodynamics Flow Over a Vertical Plate with Convective Boundary Condition

Bayo Johnson Akinbo* and Bakai Ishola Olajuwon

Department of Mathematics, Federal University of Agriculture, Abeokuta, Nigeria
E-mail: akinbomaths@gmail.com
**Corresponding Author*

Received 17 May 2021; Accepted 25 November 2021;
Publication 16 December 2021

Abstract

Heat generation effect in a steady two-dimensional magnetohydrodynamics (MHD) flow over a moving vertical plate with a medium porosity has been studied. By similarity transformation variables, the coupled non-linear ordinary differential equations describing the model are obtained. The resulting equation is then solved, using Galerkin Weighted Residual Method (GWRM), where the effect of heat generation, Magnetic Parameter as well as other physical parameters encountered were examined and discussed. Some of the major findings were that increase in heat generation and convective heat parameter enhances the plate surface temperature as well as temperature field which allows the thermal effect to penetrate deeper into the quiescent fluid.

Keywords: Similarity variables, magnetic field, heat generation/absorption, Galerkin Weighted Residual.

European Journal of Computational Mechanics, Vol. 30_4–6, 431–452.
doi: 10.13052/ejcm2642-2085.30466

1 Introduction

The phenomenon of heat generation/absorption and dissipation effect under the influence of magnetic field has practical application in various aspects of science and technological fields such as thermal insulation, combustion, and cooling of nuclear reactors (Ahmad and Khan [1]) etc. In the view of its various applications, many authors have made contributions to the literature. Whenever the heat generation occurs, the operating temperature and its layer thickness are strengthened (increased) but lower for heat absorption. Chamkha and Issa [2] reported that the temperature field and thermal layer thickness are improved (increased) via the enhancement in heat generation while investigating two-dimensional, laminar, hydromagnetic flow with heat and mass transfer over a semi-infinite, permeable flat surface in the presence of thermophoresis and heat generation or absorption. Similar reports are buttressed by Kasmani et al. [3]. Other authors like Lakshmi et al. [4], and Reddy et al. [5, 6] also considered the impact of heat generation/absorption in their investigations.

The attention of researchers had also been drawn to the viscous dissipative effect which plays an important role in both free and forced convection flows. Vagravelu and Hadjinicolaru [7] investigated heat transfer in a viscous fluid over a stretching sheet with viscous dissipation and internal heat generation and MHD-conjugate heat transfer analysis for a vertical flat plate in presence of viscous dissipation and heat generation was investigated by Mamun et al. [8]. Kabir et al. [9] and Abo-Eldahab and El-Aziz [10] considered the effect of viscous dissipation on MHD natural convection flow along a vertical surface. The interactive influence of viscous dissipation with Radiation on MHD Marangoni flow via a permeable flat surface is examined by Sreenivasulu et al. [11]. Considerable numbers of work have been done on porosity on the account of its wide application in Science related disciplines. Little among these applications include solar energy collectors, energy recovery of petroleum resource and geophysical applications etc. as a result of its wide applications, it has been studied in the literature. Soundalgekar [12] considered the unsteady-case of free convective flow through an infinite vertical porous plate with viscous dissipation and constant suction. Anajali and Ganga [13–15] imposed different conditions while investigating magnetohydrodynamics fluid with a medium porosity. The stretching porous surface is investigated with the combined impact of a chemical reaction and Viscous dissipation by Singh [16]. Sharma et al. [17] worked on natural convection magnetohydrodynamics flow on medium porosity with generation/absorption and periodic wall temperature.

Motivated by the applications and previous workdone by different authors, this particular work intends to investigate the behaviours of heat generation/absorption on Magnetohydrodynamics (MHD) flow over a vertical plate with convective boundary condition. The study is considered with a medium porosity.

2 Mathematical Formulation

Let us put into consideration the free convection, boundary-layer flow of a stream of cold of an incompressible fluid at temperature T_∞ which takes place with the interactive impact of heat generation/absorption. The outer-covering of the layer is made hot by convection arising from a hot fluid at temperature T_f which produces h_f as coefficient of heat transfer. The cold fluid in contact with the plate generates heat internally at a volumetric rate Q_0. The intensity of magnetic field B_0 transversely acts in the direction of the flow while the Joule heating influence, as well as magnetic Reynolds number, is ignored due to its negligible impact to hinder the motion of the free convection. The temperature and concentration of the fluid are considered as T and C respectively while the fluid velocity in x and y directions are respectively denoted by u and v. The $x - axis$ is considered along with the flow and $y - axis$ normal to it. C_w is the plate surface concentration while T_∞ and C_∞ denote ambient temperature and concentration respectively, as shown in Figure 1. In accordance with the above expressions via Boussinesq's approximation, the model equations can be written as

$$\frac{\partial u}{\partial x} + \frac{\partial v}{\partial y} = 0 \tag{1}$$

$$u\frac{\partial u}{\partial x} + v\frac{\partial u}{\partial y} = \nu\frac{\partial^2 u}{\partial y^2} - \frac{\sigma B_0^2 u}{\rho} - \frac{\nu}{K}u + g\beta_T(T - T_\infty) + g\,\beta_c(C - C_\infty) \tag{2}$$

$$u\frac{\partial T}{\partial x} + v\frac{\partial T}{\partial y} = \alpha\frac{\partial^2 T}{\partial y^2} + \frac{\nu}{C_p}\left(\frac{\partial u}{\partial y}\right)^2 - \frac{1}{\rho C_p}\frac{\partial q_r}{\partial y} + \frac{Q_0(T - T_\infty)}{\rho C_p} \tag{3}$$

$$u\frac{\partial C}{\partial x} + v\frac{\partial C}{\partial y} = D\frac{\partial^2 C}{\partial y^2} \tag{4}$$

Where D denotes mass diffusivity, α body forth thermal diffusivity, g represents acceleration which occurs as a result of gravity, ρ typifies density,

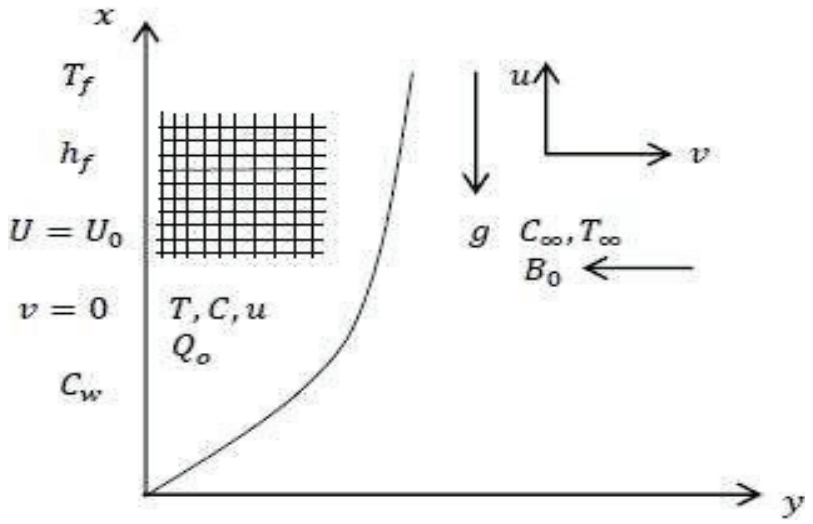

Figure 1 Flow configuration and coordinate system.

σ shows electrical conductivity, β_T and β_c respectively connotes thermal and concentration expansion coefficient, Q_0 is the volumetric heat generation/absorption coefficient, C_p denotes specific heat at constant pressure, K denotes permeability of the porous medium while ν is the kinematics viscosity, (u, v) are the components of velocity at any point (x, y). Concur with the following conditions

$$U(x,0) = U_0, \quad V(x,0) = 0, \quad -k\frac{\partial T(x,0)}{\partial y} = h_f[T_f - T(x,0)],$$

$$C_w(x,0) = Ax^\lambda + C_\infty$$

$$U(x,\infty) = 0, \quad T(x,\infty) = T_\infty, \quad C(x,\infty) = C_\infty \tag{5}$$

Here, λ connotes the index power of the concentration and k is the thermal conductivity coefficient. The radiative heat flux by Roseland was adopted and expressed (Shit and Haldar [18]) as

$$q_r = \frac{-4\sigma^*}{3k^*}\frac{\partial T^4}{\partial y} \tag{6}$$

Where k^* stands as the coefficient of the mean of absorption and σ^* typifies Sterfan-Boltzmann constant. Bearing in mind that the temperature

differences within the flow are such that Equation (6) can be linearized subjecting T^4 into Taylor series around T_∞ and disuse higher-order terms gives

$$T^4 \approx 4T_\infty^3 T - 3T_\infty^4 \tag{7}$$

By the introduction of Equations (6) and (7) in Equation (3), we have

$$u\frac{\partial T}{\partial x} + v\frac{\partial T}{\partial y} = \alpha\frac{\partial^2 T}{\partial y^2} + \frac{\nu}{C_p}\left(\frac{\partial u}{\partial y}\right)^2 + \frac{16\sigma T_\infty^3}{3k^*\rho C_p}\frac{\partial^2 T}{\partial y^2} + \frac{Q_0(T - T_\infty)}{\rho C_p} \tag{8}$$

Following Bhattacharyya et al. [19], Equation (1) is trivially satisfied through the stream function expressed by

$$u = \frac{\partial \psi}{\partial y} \quad \textit{and} \quad v = -\frac{\partial \psi}{\partial x} \tag{9}$$

Invoking

$$\eta = y\sqrt{\frac{U_0}{\nu x}}, \quad \psi = \sqrt{\nu x U_0} f(\eta), \tag{10}$$

where U_0 connotes the velocity of the plate and,

$$\theta(\eta) = \frac{T - T_\infty}{T_f - T_\infty}, \quad \emptyset(\eta) = \frac{C - C_\infty}{C_w - C_\infty} \tag{11}$$

Body-forth non-dimensional; temperature and concentration. Applying Equations (9)–(11) into Equations (1)–(2), (4)–(5), and modified Equation (8), we have

$$\frac{d^3 f(\eta)}{d\eta^3} + \frac{1}{2} f(\eta)\frac{d^2 f(\eta)}{d\eta^2} - (Ha + P_s)\frac{df(\eta)}{d\eta} + Gr\theta(\eta) + Gc\emptyset(\eta) = 0 \tag{12}$$

$$\left(1 + \frac{4}{3Ra}\right)\frac{d^2\theta(\eta)}{d\eta^2} + PrEc\left(\frac{d^2 f(\eta)}{d\eta^2}\right)^2 + \frac{1}{2}Prf(\eta)\frac{d\theta(\eta)}{d\eta} + Q\theta(\eta) = 0 \tag{13}$$

$$\frac{d^2\emptyset(\eta)}{d\eta^2} + \frac{1}{2}Scf(\eta)\frac{d\emptyset(\eta)}{\partial\eta} = 0 \tag{14}$$

Where the derivatives are considered with respect to η and

$$Ha = \frac{\sigma B_0^2 x}{\rho U_0}, \quad Gr = \frac{g\beta_T(T_f - T_\infty)x}{U_0^2}, \quad Gc = \frac{g\beta_c(C_w - C_\infty)x}{U_0^2},$$

$$Bi = \frac{hf}{k}\sqrt{\frac{\nu x}{U_0}}, \quad \alpha = \frac{k^*}{\rho C_\rho}$$

$$P_s = \frac{\nu x}{KU_0}, \quad Pr = \frac{\nu}{\alpha}, \quad Sc = \frac{\nu}{D}, \quad Q = \frac{xQ_0\nu}{\rho C_p U_0},$$

$$Ec = \frac{U_0^2}{C_p(T_f - T_\infty)}, \quad Ra = \frac{kk^*}{4\sigma^* T_\infty^3} \tag{15}$$

where Ha represents local magnetic parameter, (Gr, Gc) shows local thermal and solutal Grashof number respectively, Bi stands for local convective heat parameter (or Boit number), Pr portrays Prandtl number, Sc body–forth Schmidt number, P_s connotes local Porosity parameter, Q denotes local heat generation/absorption parameter, Ec stands for Eckert number while Ra typifies Radiation parameter. Agreed with the following boundary conditions

$$f(0) = 0, \quad f'(0) = 1, \quad \theta'(0) = Bi[\theta(0) - 1], \quad \emptyset(0) = 1 \tag{16}$$

$$f'(\infty) = 0, \quad \theta(\infty) = 0, \quad \emptyset(\infty) = 0 \tag{17}$$

Following Lakshmi et al. [20] by keeping in mind the local parameters Bi, Ha, Gr, Gc, Q and P_s in (12)–(14) are functions of x. We obtained the similarity solution by holding on to the following parameters

$$h_f = \frac{a}{\sqrt{x}}, \quad \sigma = \frac{b}{x}, \quad \beta_T = \frac{c}{x},$$

$$\beta_c = \frac{d}{x}, \quad Q_0 = \frac{e}{x}, \quad K = \frac{x}{q} \tag{18}$$

Where a, b, c, d, e and q are constants taken with the right dimension. The transformed equations which agreed with the conditions of Equations (16) and (17) are solved by Galerkin Weighted Residual Method as shown in (3.0) below. Due to Engineering application, we respectively considered the local skin friction, as well as Local Nusselt and local Sherwood numbers as;

$$C_f = \frac{2\tau_w}{\rho U_0^2}, \quad Nu = \frac{xq_w}{k(T_f - T_\infty)} \quad \text{and} \quad Sh = \frac{xq_m}{D(C_w - C_\infty)} \tag{19}$$

Which gives

$$Re_x^{\frac{1}{2}} C_f = f''(0), \quad Re_x^{-\frac{1}{2}} Nu = -\left(1 + \frac{4}{3Ra}\right)\theta'(0) \quad \text{and}$$

$$Re_x^{-\frac{1}{2}} Sh = -\emptyset'(0) \tag{20}$$

Where $Re_x = U_0 x/\nu$ represents Reynold number, τ_w acts as shear stress on the plate, q_w body forth the surface heat while q_m expresses the surface mass.

3 Method of Solution

Non-linear differential equations are practically crucial in mathematical modeling. They can be tackled via different methods, such as; Adomian Decomposition, Homotopy perturbation, and so on. Galerkin Weighted Residual Method (GWRM) is chosen over others due to its efficiency to provide accurate results while dealing with the coupled higher-order differential equations. In agreement with Oderinu and Aregbesola [21], from Equations (12)–(14) and (16)–(17), we assumed the trial functions

$$f = \sum_{i=0}^{12} a_i e^{-\frac{i\eta}{4}}, \quad \theta = \sum_{i=1}^{13} b_i e^{-\frac{i\eta}{4}}, \quad \emptyset = \sum_{i=1}^{13} c_i e^{-\frac{i\eta}{4}} \tag{21}$$

Imposing the boundary conditions (15), we have

$$a_0 + a_1 + a_2 + a_3 + a_4 + a_5 + a_6 + a_7 + a_8 + a_9 + a_{10} + a_{11} + a_{12} = 0 \tag{22}$$

$$b_1 + b_2 + b_3 + b_4 + b_5 + b_6 + b_7 + b_8 + b_9 + b_{10} + b_{11} + b_{12} + b_{13} - 1 = 0 \tag{23}$$

$$c_1 + c_2 + c_3 + c_4 + c_5 + c_6 + c_7 + c_8 + c_9 + c_{10} + c_{11} + c_{12} + c_{13} - 1 = 0 \tag{24}$$

and for $f'(0) = 1$, $\theta'(0) = Bi[\theta(0) - 1]$, we have

$$-\frac{1}{4}a_1 - \frac{1}{2}a_2 - \frac{3}{4}a_3 - a_4 - \frac{5}{4}a_5 - \frac{3}{2}a_6 - \frac{7}{4}a_7 - 2a_8 - \frac{9}{4}a_9 - \frac{5}{2}a_{10} - \frac{11}{4}a_{11} - 3a_{12} - 1 = 0 \tag{25}$$

$$
\begin{aligned}
&-\left(\frac{1}{4}+Bi\right)b_1-\left(\frac{1}{2}+Bi\right)b_2-\left(\frac{3}{4}+Bi\right)b_3\\
&\quad-(1+Bi)\,b_4-\left(\frac{5}{4}+Bi\right)b_5\\
&-\left(\frac{3}{2}+Bi\right)b_6-\left(\frac{7}{4}+Bi\right)b_7-(2+Bi)\,b_8\\
&\quad-\left(\frac{9}{4}+Bi\right)b_9-\left(\frac{5}{2}+Bi\right)b_{10}\\
&\quad-\left(\frac{11}{4}+Bi\right)b_{11}-(3+Bi)\,b_{12}-\left(\frac{13}{4}+Bi\right)b_{13}+Bi=0
\end{aligned}
\tag{26}
$$

Equation (17) automatically agreed. In accordance with the rule of the solution, the application of Equations (21) and (12)–(14) give the residual functions R_f, R_θ and $R_\emptyset$ (See Oderinu and Aregbesola [21]) which are multiplied by $e^{-\frac{j}{4}\eta}\forall\, j \in \mathbb{Z}$, and successfully integrated under the domain. Here, the algebraic equations emanated are tackled with the computer MATHEMATICA package, and the results obtained are discussed accordingly.

4 Validation of the Study

Implementation of numerical computation with the previous workdone was first considered by comparing it with the results with Makinde [22] by setting $P_s = 0, Q = 0, Ra = 0, Ec = 0$. The results are found to be in excellent agreement as displayed in Table 1.

Table 2 present the behaviours of each parameter encountered for local skin-friction, local Nusselt number, Plate surface temperature, and local Sherwood number. Various values of each parameter quantitatively displayed negative for the local skin-friction, demonstrating the presence of a drag force exerted on the fluid by the plate. The Nusselt number improves for different values of convective heat parameter (Bi), and Prandt number (Pr) which consequently boosts the rate of heat transfer with reverse phenomenon on Eckert number (Ec), Radiation parameter (Ra) and heat generation parameter (Q). In addition, the Sherwood number increases with various values Schmidt number which in turn enhances the rate of mass transfer.

Table 1 The present result with Makinde [22]

						Makinde [22]				Present Result			
Ha	Gr	Gc	Bi	Pr	Sc	$f''(0)$	$-\theta'(0)$	$\theta(0)$	$-\emptyset'(0)$	$f''(0)$	$-\theta'(0)$	$\theta(0)$	$-\emptyset'(0)$
0.1	0.1	0.1	0.1	0.72	0.62	−0.402271	0.078635	0.213643	0.3337425	−0.402270	0.078634	0.213636	0.3337431
1.0	0.1	0.1	0.1	0.72	0.62	−0.352136	0.273153	0.726846	0.3410294	−0.352135	0.273152	0.726839	0.3410288
10	0.1	0.1	0.1	0.72	0.62	−0.329568	0.365258	0.963474	0.3441377	−0.329567	0.365256	0.963473	0.3441369
0.1	0.5	0.1	0.1	0.72	0.62	−0.322212	0.079173	0.208264	0.3451301	−0.322211	0.079172	0.208261	0.3451300
0.1	1.0	0.1	0.1	0.72	0.62	−0.231251	0.079691	0.203088	0.3566654	−0.231250	0.079690	0.203085	0.3566647
0.1	0.1	0.5	0.1	0.72	0.62	−0.026410	0.080711	0.192889	0.3813954	−0.026408	0.080710	0.192887	0.3813960
0.1	0.1	1.0	0.1	0.72	0.62	0.3799184	0.082040	0.179592	0.4176697	0.379917	0.082035	0.179590	0.4176695
0.1	0.1	0.1	1.0	0.72	0.62	−0.985719	0.074174	0.258252	0.2598499	−0.985718	0.074173	0.258251	0.2598501
0.1	0.1	0.1	5.0	0.72	0.62	−2.217928	0.066156	0.338435	0.1806634	−2.217927	0.066154	0.338429	0.1806631
0.1	0.1	0.1	0.1	1.00	0.62	−0.407908	0.081935	0.180640	0.3325180	−0.407907	0.081935	0.180637	0.3325176
0.1	0.1	0.1	0.1	7.10	0.62	−0.421228	0.093348	0.066513	0.3305618	−0.421227	0.093352	0.066512	0.3305617
0.1	0.1	0.1	0.1	0.72	0.78	−0.411704	0.078484	0.215159	0.3844559	−0.411703	0.078482	0.215158	0.3844556

Table 2 Significant embedded parameter on Skin-friction, Nusselt number, plate surface temperature, and Sherwood number

Ha	Gr	Gc	Bi	Ec	P_s	Q	Pr	Sc	Ra	$Re_x^{\frac{1}{2}} C_f$	$Re_x^{-\frac{1}{2}} Nu$	$\theta(0)$	$Re_x^{-\frac{1}{2}} Sh$
0.1	0.1	0.1	0.1	0.1	0.1	0.01	0.72	0.62	0.7	−0.451814	0.171544	0.409439	0.331231
0.5										−0.738708	0.152685	0.474363	0.290705
1.0										−1.004783	0.133322	0.541023	0.256780
	0.5									−0.273902	0.185819	0.360297	0.364958
	1.0									−0.095755	0.193427	0.334104	0.390016
		0.5								−0.098393	0.186019	0.359606	0.375238
		1.0								0.294958	0.193073	0.335323	0.410769
			0.5							−0.405655	0.354037	0.756237	0.341324
			1.0							−0.392376	0.410588	0.858650	0.343997
				1.0						−0.423552	0.120890	0.583823	0.338065
				3.0						−0.374099	0.031522	0.891482	0.348926
					0.5					−0.738708	0.152685	0.474363	0.290705
					1.0					−1.004783	0.133322	0.541023	0.256780
						0.04				−0.434812	0.148154	0.489963	0.336591
						0.07				−0.402381	0.103994	0.641997	0.346015
							1.0			−0.464224	0.187231	0.355435	0.326853
							3.0			−0.489839	0.224686	0.226490	0.318814
								0.24		−0.420466	0.178641	0.385006	0.180222
								0.78		−0.459254	0.170221	0.413994	0.382780
									2.0	−0.470403	0.111995	0.328028	0.324677
									3.0	−0.474379	0.099781	0.309208	0.323346

5 Discussion of Results

In this paper, the dimensionless Equations (12)–(14) with the conditions (16) and (17) are executed via Galerkin Weighted Residual method. The resulting effects of various parameters are discussed as follows

The Schmidt number Sc with respect to air is taken to be $Sc = 0.24\ (H_2)$, $0.62\ (H_2O)$, $Sc = 0.78\ (NH_3)$ and $Sc = 2.62\ (C_9H_{12})$ while the value of Prandtl number to air is considered as 0.72. Other parameters were discussed by keeping $Gr = 0.1$, $Gc = 0.1$, $Bi = 0.1$, $Ec = 0.1$, $P_s = 0.1$, $Ha = 0.1$, $Sc = 0.62$, $Pr = 0.72$, $Q = 0.01$ and $Ra = 0.7$ constant for each varying parameter.

Figures 2–3 reveal the output of Magnetic impact Ha via velocity and temperature fields respectively. It is obvious from the Figure 2 as expected that the velocity impact across the layer thins as $Ha > 0$. This is true as an increase in magnetic strength brings about an opposing force to the flow called Lorentz-force which has tendency to impede the motion of the fluid and decrease the associated layer thickness. However, the effects of Lorentz force pioneer frictional-heating which in turns magnifies the temperature across the layer and boosts the thermal boundary layer thickness.

The behaviors of thermal Grashof number (Gr) and Solutal Grashof number (Gc) are presented in Figures 4–7. The presence of $Gr > 0$ and $Gc > 0$ accelerates the motion of the fluid, which in turn enhances the

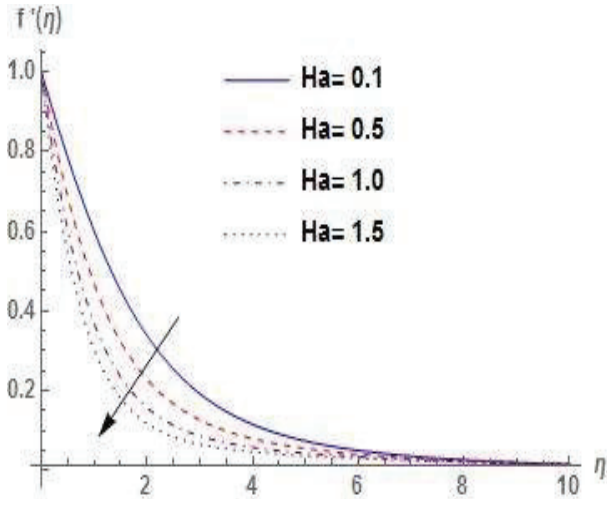

Figure 2 Significance of Ha on Velocity $f'(\eta)$.

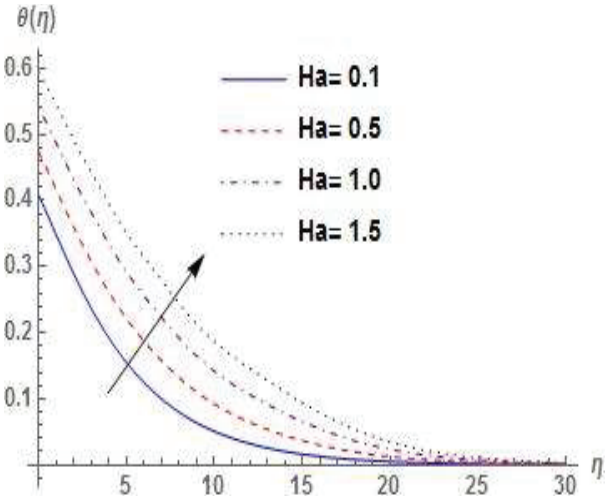

Figure 3 Significance of Ha on temperature $\theta(\eta)$.

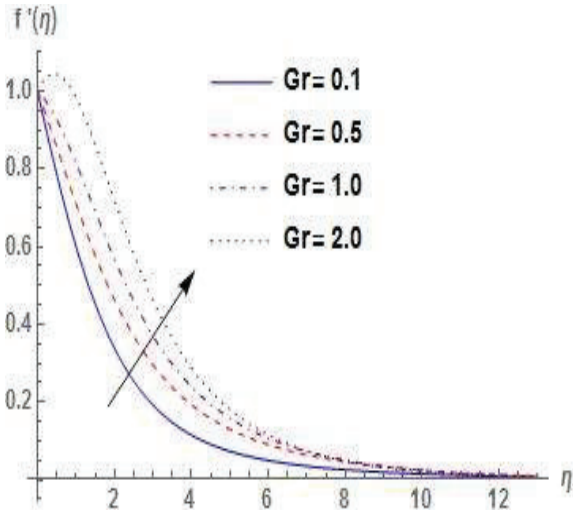

Figure 4 Significance of Gr on Velocity $f'(\eta)$.

momentum boundary layer thickness. On the other hand, various values of Gr and Gc as demonstrated in Figures 5 and 6 decline the temperature and concentration fields (profiles) which consequently thins thermal and concentration boundary layer thickness. It is noteworthy that $Gr > 0$, and $(Gc > 0)$ cools the surface (See Table 2) and show at the plate surface

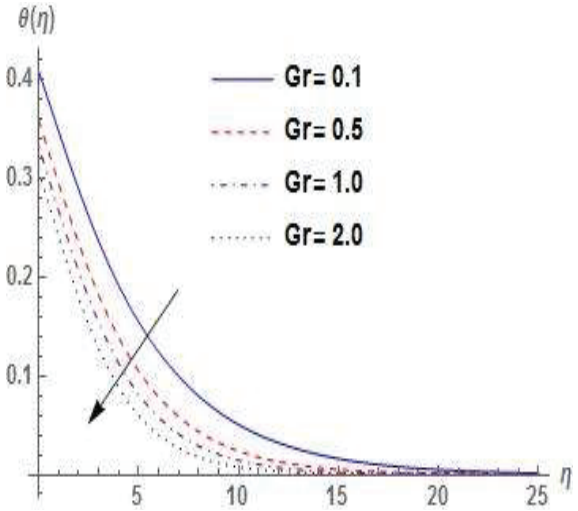

Figure 5 Significance of Gr on temperature $\theta(\eta)$.

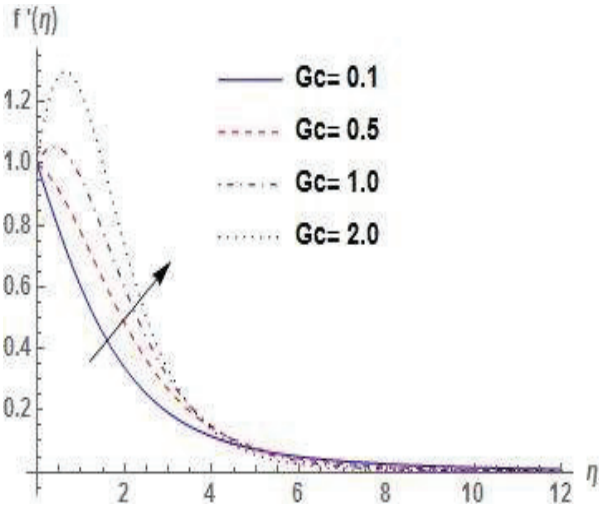

Figure 6 Significance of Gc on Velocity $f'(\eta)$.

that concentration is more effective in comparison with the free stream respectively. The cooling surface among which is a nuclear reactor frequently experience in application in this scientific driven World.

The significance of Prandtl number Pr on temperature profile is presented in Figure 8. An increase in Pr on the basis of low thermal diffusivity

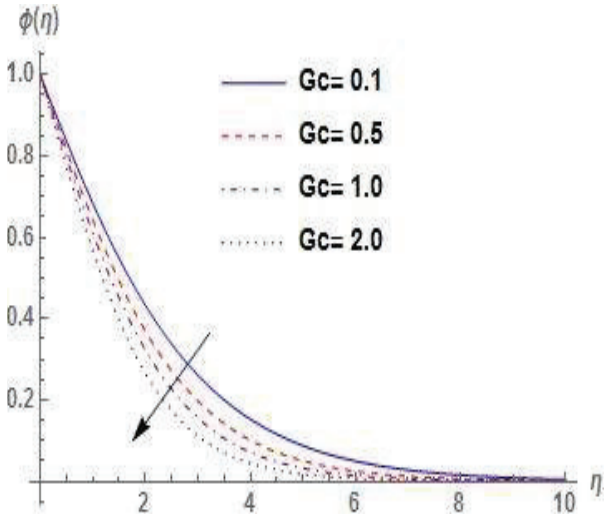

Figure 7 Significance of Gc on concentration $\emptyset(\eta)$.

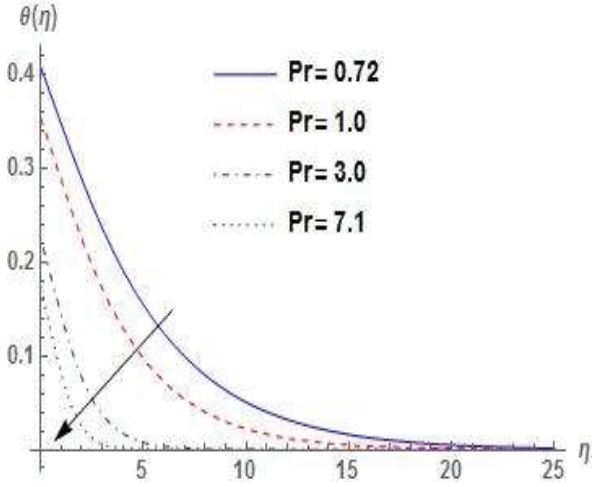

Figure 8 Significance of Pr on Temperature $\theta(\eta)$.

escalates Nusselt number and improves the surface heat transfer as shown in Table 2. In addition, maximum values of Pr lessen the temperature impact across the layer which ultimately declines its layer thickness. Hence, thermal conductivity is inflated at smaller values of Pr thereby enable the heat to diffuse more quickly from the heated surface in comparison with the higher values. However, the presence of Schmidt number $(Sc > 0)$ which

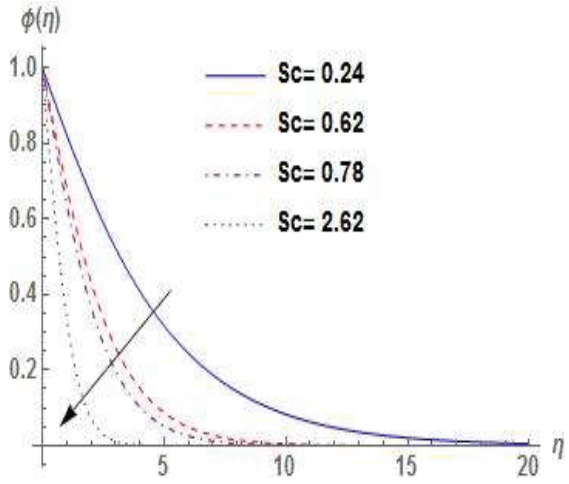

Figure 9 Significance of Sc on concentration $\emptyset(\eta)$.

is traceable to low molecular-diffusivity, demoralizes diffusion properties of the fluid which consequently reduces the concentration profile and lower concentration boundary layer thickness. Moreover, the Sherwood number improves with large values of (Sc) and boosts the rate of mass transfer (See Figure 9).

From Figure 10, it is viewed that the fluid molecule improves with large values of heat generation parameter Q. This in turn enhances the operating temperature and strengthens the thermal boundary layer thickness. Thus, large values of Q enable the penetrations of the thermal strength to the quiescent fluid. The behaviors of Eckert number (Ec) on temperature profile are presented in Figure 11. (Ec) expresses the transformation of kinetic into internal energy by workdone against the viscous-fluid stresses. However, large values of Ec increase the temperature distribution which strengthens thermal layer thickness.

The effect of radiation parameter (Ra) on temperature field is presented in Figure 12. An increase in Ra pioneered reduction in the rate of energy transport to the fluid (Ouaf [23]), owing to the presence of radiation term in the denominator of the energy equation. This ultimately declines the temperature field and compresses its layer thickness. In Figure 13, the temperature distribution and associated layer thickness notably experience greater boosts to its peak for large values of convective heat parameter (Bi). This occurs as a result of the left-surface of the plate that is exposed to the hot-fluid thereby

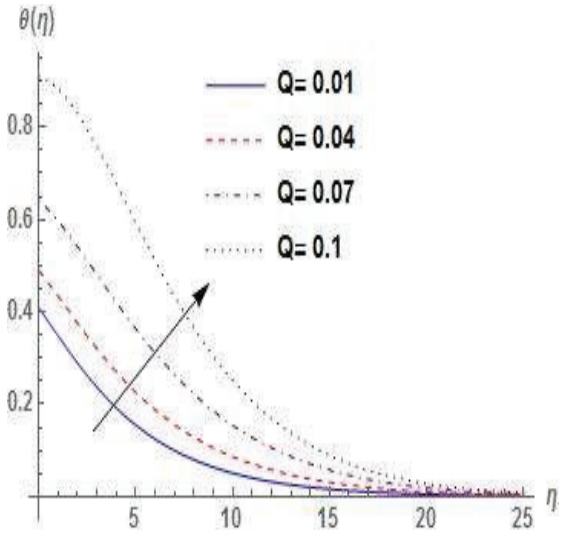

Figure 10 Significance of Q on Temperature $\theta(\eta)$.

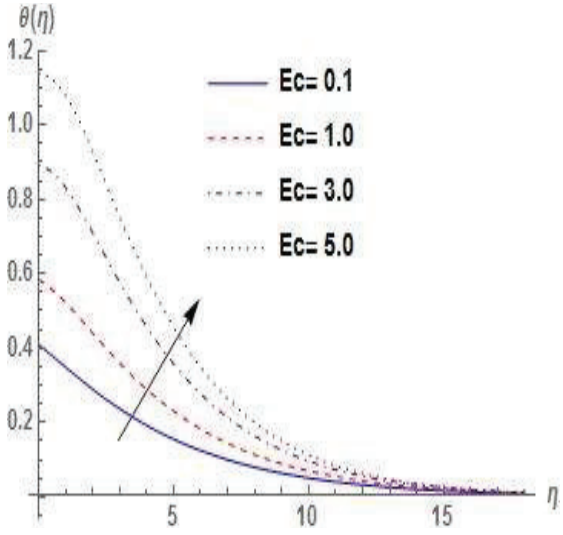

Figure 11 Significance of Ec on Temperature $\theta(\eta)$.

making the right-surface to be lighter and flow faster. However, Nusselt number is greatly enhanced with the interaction of $(Bi > 0)$ which in turn strengthens the surface heat transfer.

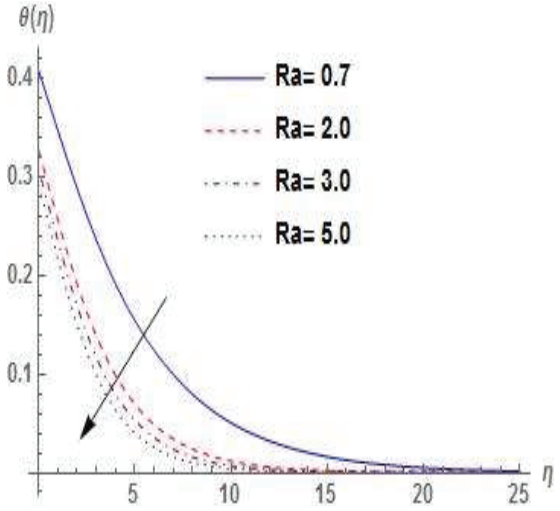

Figure 12 Significance of Ra on Temperature $\theta(\eta)$.

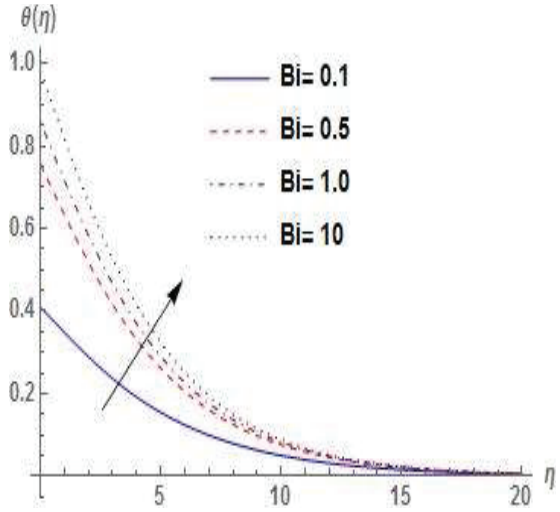

Figure 13 Significance of Bi on Temperature $\theta(\eta)$.

Figures 14–15 depict the behaviors of Porosity on velocity and temperature profiles. Increase in P_s pioneer resistance to the motion of the fluid, which in turn decreases the velocity distribution within the boundary layer

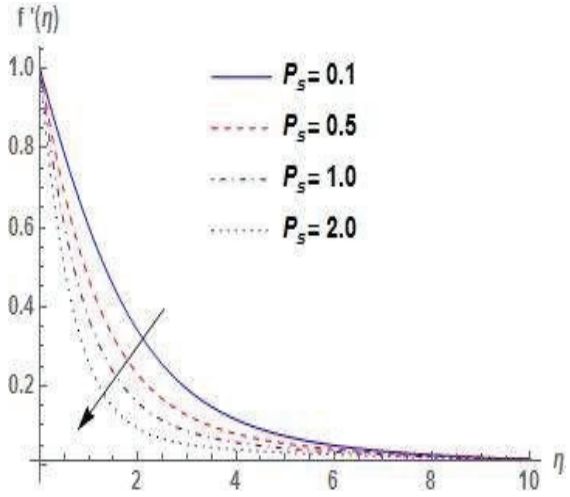

Figure 14 Significance of P_s on Velocity $f'(\eta)$.

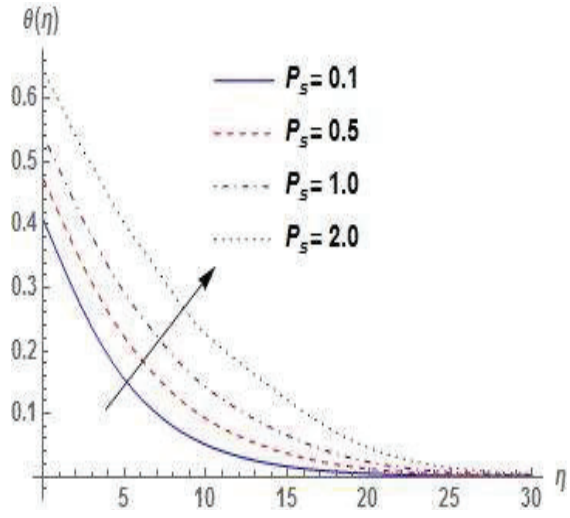

Figure 15 Significance of P_s on temperature $\theta(\eta)$.

and its layer thickness. However, the fluid molecules are disturbed via $P_s > 0$ which stirred-up heat within the layer that enhances the temperature field and its layer thickness.

6 Conclusion

In this paper, the computation techniques are engaged to study the effects of heat generation on heat and mass transfer in Magnetohydrodynamics (MHD) flow over a vertical plate embedded in a porous medium with convective boundary condition. The model equations for transport phenomenon are performed via Galerkin Weighted Residual method and the results are discussed accordingly with the following crucial point among other obtained

- ➢ the Cooling problem which is often encountered in engineering applications such as cooling of electronic components and nuclear reactors is guaranteed with the positive values of thermal Grashof number
- ➢ The rate of heat transfer is magnified on increase in heat generation parameter, thereby causes an increase in fluid temperature.
- ➢ The interaction of Magnetic parameter pioneer frictional heating within the layer thereby results in an increase in fluid temperature
- ➢ The fluid temperature overshoots with a rise in heat generation and convective heat parameter, often used in Science related fields for drying of materials.

References

[1] R. Ahmad, and W. A. Khan. Effect of viscous dissipation and internal heat generation/absorption on heat transfer flow over a moving wedge with convective boundary condition. *Heat Transfer – Asian Research*, 42(7): 589–602, 2013.

[2] A. J. Chamkha and C. Issa. Effects of heat generation/absorption and thermophoresis on hydromagnetic flow with heat and mass transfer over a flat surface. *International Journal of Numerical Methods for Heat and Fluid Flow*. 10(4): 432–448, 2000.

[3] R. M. Kasmani, S. Sivasankaran, M. Bhuvaneswari, Z. Siri. Effect of chemical reaction on convective heat transfer of boundary layer flow in nanofluid over a wedge with heat generation/absorption and suction. *Journal of Applied Fluid Mechanics*, 9(1): 379–388, 2016.

[4] K. B. Lakshmi, G. S. S. Raju, P. M. Kishore, N. V. R. V. P. Rao. The study of heat generation and viscous dissipation on MHD heat and mass diffusion flow past a surface. *Journal of applied physics*, 5(4): 17–28, 2013.

[5] N. B. Reddy, T. Poornima, P. Sreenivasulu. Internal heat generation and viscous dissipation effects on nanofluids over a moving vertical

plate with convective boundary condition. *International Conference on Frontiers in Mathematics*, 123–129, 2015.

[6] M. G. Reddy, P. Padma, B. Shankar. Effects of viscous dissipation and heat source on unsteady MHD flow over a stretching sheet. *Ain Shams Engineering Journal*, 6(4): 1195–1201, 2015.

[7] K. Vajravelu, A. Hadjinicolaou. Heat transfer in a viscous fluid over a stretching sheet with viscous dissipation and internal heat generation. *International Communications in Heat and Mass Transfer*, 20(3): 417–430, 1993.

[8] A. A. Mamun, Z. R. Chowdhury, M. A. Azim, M. M. Molla. MHD-conjugate heat transfer analysis for a vertical flat plate in presence of viscous dissipation and heat generation. *International Communications in Heat and Mass Transfer*, 35(10): 1275–1280, 2008.

[9] K. H. Kabir, M. A. Alim, L. S. Andallah. Effect of viscous dissipation on MHD natural convection flow along a vertical wavy surface with heat generation. *America Journal of Computational Mathematics*, 3: 91–98, 2013.

[10] Abo-Eldahab, E. M., El-Aziz, M. A., Viscous dissipation and Joules heating effects on MHD-free convection from a vertical plate with power-law variation in surface temperature in the presence of hall and ion-slip currents. *Applied Mathematical Modelling*, 29(6): 579–595, 2005.

[11] P. Sreenivasulu, N. B. Reddy, M. G. Reddy. Radiation and viscous dissipation effects on steady MHD Marangoni convection flow over a permeable flat surface with heat generation or absorption. *International Journal of Mathematical Archives*, 4(2): 174–183, 2013.

[12] V. M. Soundalgekar. Viscous dissipation effects on unsteady free convective flow past an infinite vertical porous plate with constant suction. International Journal of Heat and Mass Transfer, 15(6): 1253–1261, 1972.

[13] S. P. A. Devi, B. Ganga. Effects of Viscous and Joules dissipation on MHD flow,haet and mass transfer past a stretching porous surface embedded in a porous medium. *Nonlinear Analysis: Modelling and Control*, 14(3): 303–314, 2009.

[14] S. P. A. Devi, B. Ganga. Viscous dissipation effects on nonlinear MHD flow in a porous medium over a stretching porous surface. *International Journal of Applied Mathematics and Mech.*, 5(7): 45–59, 2009.

[15] S. P. A. Devi, B. Ganga. Dissipation effect on MHD flow and heat transfer past a porous surface with prescribed heat flux. *Journal of Applied Fluid Mechanics*, 3(1): 1–6, 2010.

[16] J. Singh. Viscous dissipation and chemical reaction effects on flow past a stretching porous surface in a porous medium. *Adv. Theor. Appl. Mech*., 5(8): 323–331, 2012.

[17] P. R. Sharma, K. Sharma, T. Mehta. Radiative and free convective effects on MHD flow through a porous medium with periodic wall temperature and heat generation or absorption. *International journal of mathematical archive*, 5(9): 119–128, 2014.

[18] G. C. Shit, R. Haldar. Effects of thermal radiation on MHD viscous fluid flow and heat transfer over nonlinear shrinking porous sheet. Applied Mathematics and Mechanics, 32: 677–688, 2011.

[19] K. Bhattacharyya, S. Mukhopadhyay, G. C. Layek. Slip effects on boundary layer stagnation-point flow and heat transfer towards a shrinking sheet. *International Journal of Heat and Mass transfer*, 54: 308–313, 2011.

[20] R. Lakshmi, K. R. Jayarami, K. Ramakrishna, G. V. R. Reddy. Numerical Solution of MHD flow over a moving vertical porous plate with heat and Mass Transfer. *Int. J. Chem.sci.*, 12: 1487–1499, 2014.

[21] R. A. Oderinu, Y. A. S. Aregbesola. Weighted Residual method in a semi-infinite domain using un-partitioned methods. *Int., Jour., of Applied Mathematics*, 25(1), 25–31, 2012.

[22] O. D. Makinde. On MHD heat and Mass Transfer over a moving vertical plate with a convective surface boundary condition. *Can. J. Chem. Eng*. 88: 983–990, 2010.

[23] M. E.M. Ouaf. Exact solution of thermal radiation on MHD flow over a stretching porous sheet. *Applied Mathematics and Computation*, 170: 1117–1125, 2005.

Biographies

Bayo Johnson Akinbo (B.Sc[Ed]., M.Sc., Ph.D) is a Researcher at Federal University of Agriculture, Abeokuta, Nigeria. His area of research involves Fluid Mechanics and Mathematical Modeling.

Bakai Ishola Olajuwon (B.Sc., M.Tech., Ph.D) is a Professor and Researcher at Federal University of Agriculture, Abeokuta, Nigeria. His area of research involves Fluid Mechanics and Mathematical Modeling.